



ELSEVIER

Available online at www.sciencedirect.com

SCIENCE @ DIRECT®

Journal of Colloid and Interface Science ●●● (●●●●) ●●●-●●●

JOURNAL OF  
Colloid and  
Interface Science

www.elsevier.com/locate/jcis

# Intrinsic viscosity of SiO<sub>2</sub>, Al<sub>2</sub>O<sub>3</sub> and TiO<sub>2</sub> aqueous suspensions

F.J. Rubio-Hernández\*, M.F. Ayúcar-Rubio, J.F. Velázquez-Navarro, F.J. Galindo-Rosales

*Rheology and Electrokinetics Group, Department of Applied Physics II, University of Málaga, E-29013 Málaga, Spain*

Received 30 September 2005; accepted 7 January 2006

## Abstract

The viscosity of dilute suspensions of several metal oxides (SiO<sub>2</sub>, Al<sub>2</sub>O<sub>3</sub> and TiO<sub>2</sub>) was measured at different pH values. The intrinsic viscosity,  $[\eta]$ , was derived from the concentration dependence of the viscosity. This magnitude was pH-dependent. A correlation with the shape of the kinetic unity has been proposed.

© 2006 Published by Elsevier Inc.

**Keywords:** Intrinsic viscosity; Suspensions; Oxides; Colloids; Electroviscous effects

## 1. Introduction

Experimentally it has been found that the viscosity of a very dilute colloidal suspension is linearly dependent on the solid volume fraction [1–4]. The viscosity of a dilute suspension is higher than that of the fluid phase due to two main contributions. Firstly, the presence of the particles distorts the flow field, which gives place to an increase in the dissipation of energy. Secondly, the distortion of the electrical double layer that surrounds the particles supposes an additional dissipation energy [5]. An expression that groups both effects was proposed time ago [6],

$$\eta = \eta_0(1 + [\eta](1 + p)\phi). \quad (1)$$

In this equation  $\eta$  is the viscosity of the suspension,  $\eta_0$  the viscosity of the liquid phase,  $[\eta]$  the intrinsic viscosity,  $p$  the primary electroviscous coefficient, and  $\phi$  is the solid volume fraction in the suspension. The primary electroviscous coefficient mainly depends on the electrical state at the solid–liquid interface, and the intrinsic viscosity is mainly determined by the geometry of the suspended particles. For example, Einstein [7] obtained, from theoretical considerations, that  $[\eta] = 2.5$  for spherical particles. For other particle shapes, it is obtained  $[\eta] > 2.5$  [6].

Generally, it has been accepted that the electrical state of the solid–liquid interface has no influence on the value of the  $[\eta]$  parameter. However, the variation of the inter-particle interactions due to, for example, the decrease of its repulsive electrical energy, such as it is established by the DLVO theory [8,9], gives place to the formation of aggregates (clusters) of particles. Then the kinetic unity is a cluster of particles instead of a single particle, and the  $[\eta]$  parameter should consequently change. This argument was used time ago [10], but in that case was the shear rate the magnitude of which promoted the formation of clusters. In this paper we will determine the influence of the variation of the repulsive energy between particles on the intrinsic viscosity of several oxide suspensions.

The paper is organised as follows: In the following section the experimental setup is described and in Section 3 the experimental results are discussed.

## 2. Experimental

The titanium oxide (anatase) was supplied as a white powder by Aldrich. The material (purity of 99.9%) was used without any further purification. As pointed out by Gustafsson et al. [11], attempts to further purification of the powder led to contamination. Electron microscopy (JEOL JSM840 scanning microscope) showed that the particles are roughly spherical with a mean diameter of  $200 \pm 10$  nm. The apparent specific surface area<sub>BET</sub> of these particles was determined by N<sub>2</sub> ad-

\* Corresponding author.

E-mail address: fjrubio@uma.es (F.J. Rubio-Hernández).

1 Table 1  
2 Physical and chemical properties of the suspensions

3 Material	4 Shape	5 Size (nm)	6 Area <sub>BET</sub> (m <sup>2</sup> /g)	pH <sub>IEP</sub>
SiO <sub>2</sub>	Spherical	7 ± 2	390	4.3
Al <sub>2</sub> O <sub>3</sub>	Irregular	100 ± 10	142	9.1
TiO <sub>2</sub>	Spherical	200 ± 10	10	3.5

3 sorption at 77 K by using an Autosorb-1 (Quanta Chrome)  
4 apparatus, the result being 10 m<sup>2</sup>/g.

5 The alumina used here was  $\gamma$ -Al<sub>2</sub>O<sub>3</sub> manufactured by the  
6 Goodfellow Cambridge Ltd. (England). This material is pre-  
7 sented as a powder with a purity of 99.995%. In order to remove  
8 soluble salts and other impurities, the alumina was dialysed  
9 in deionised water for 7 days, with the deionised water being  
10 changed at the beginning and end of each day [12]. There-  
11 after, the alumina suspension underwent sedimentation for 24 h.  
12 The suspension thus obtained was filtered through a filter with  
13 a pore size of 0.1  $\mu$ m and dried in order to store it in dry form  
14 to avoid contamination from trace impurities from electrolytes  
15 or water and soluble silicate. The shape and morphology of the  
16 alumina particles were determined by electron microscopy. The  
17 images showed that the particles are highly ordered crystalline  
18 grains with distinct planar faces and irregular forms. The appar-  
19 ent specific surface area<sub>BET</sub> of these particles was 142 m<sup>2</sup>/g.

20 Silica fumed (Sigma-Aldrich) was used in this work as was  
21 supplied by the manufacturer. The purity of this powder was  
22 99.8%. The primary particles are spherical with a diameter 7 ±  
23 2 nm. The apparent specific surface area<sub>BET</sub> of these particles  
24 was 390 m<sup>2</sup>/g.

25 The IEP is defined as the pH value in which the electrokinetic  
26 or  $\zeta$ -potential takes zero value. The determination of this  
27 parameter was accomplished by measuring the electrophoretic  
28 mobility of the suspensions, and converting this magnitude  
29 to  $\zeta$ -potential with Ohshima equation [13]. The results corre-  
30 sponding to the oxides here studied are shown in Figs. 1a–1c.  
31 As can be seen in Table 1, the IEP is basic for alumina and  
32 acidic for anatase and silica. Other properties of the particles  
33 have been summarised in the same Table 1.

34 All chemicals were of A.R. quality. The water was purified  
35 by reverse osmosis followed by percolation through charcoal  
36 and mixed bed ion exchange resins (Millipore).

37 The  $\zeta$ -potentials were calculated from electrophoretic mo-  
38 bility data. The electrophoretic mobilities were measured with  
39 a Zetasizer 2000 (Malvern Instruments) by taking the average  
40 of at least six measurements at the stationary level in a rectan-  
41 gular cell.

42 The viscosity of the suspensions was determined with an  
43 Ubbelohde-type (Schött-Gerate) capillary viscometer for dilu-  
44 tion, and a rheometer Rheostress RS600 (Haake). The capil-  
45 lary viscometer was calibrated using deionised water at 20, 25  
46 and 40 °C for the determination of the constants of the appar-  
47 tus. The average maximum shear rate of the viscometers was  
48 230 s<sup>-1</sup>. Starting from a fixed volume (15 ml) of the initial  
49 sample, the volume fraction of the particles was varied by dilu-  
50 ting in 5 ml steps with the same liquid phase present in the  
51 suspension. In the case of suspensions with a fixed pH, initial  
52 and final pH values of the suspensions were measured and the  
53 mean value was taken. Although a dependence of the pH on  
54 the volume fraction exists, which results from the adsorption of  
55 potential-determining ions onto the surface of the particles, it  
56 was not appreciable at these low  $\phi$  variations, the deviation be-  
57 tween initial and final pH values being less than 1%. As the ef-  
fect of the presence of the particles on the suspension viscosity

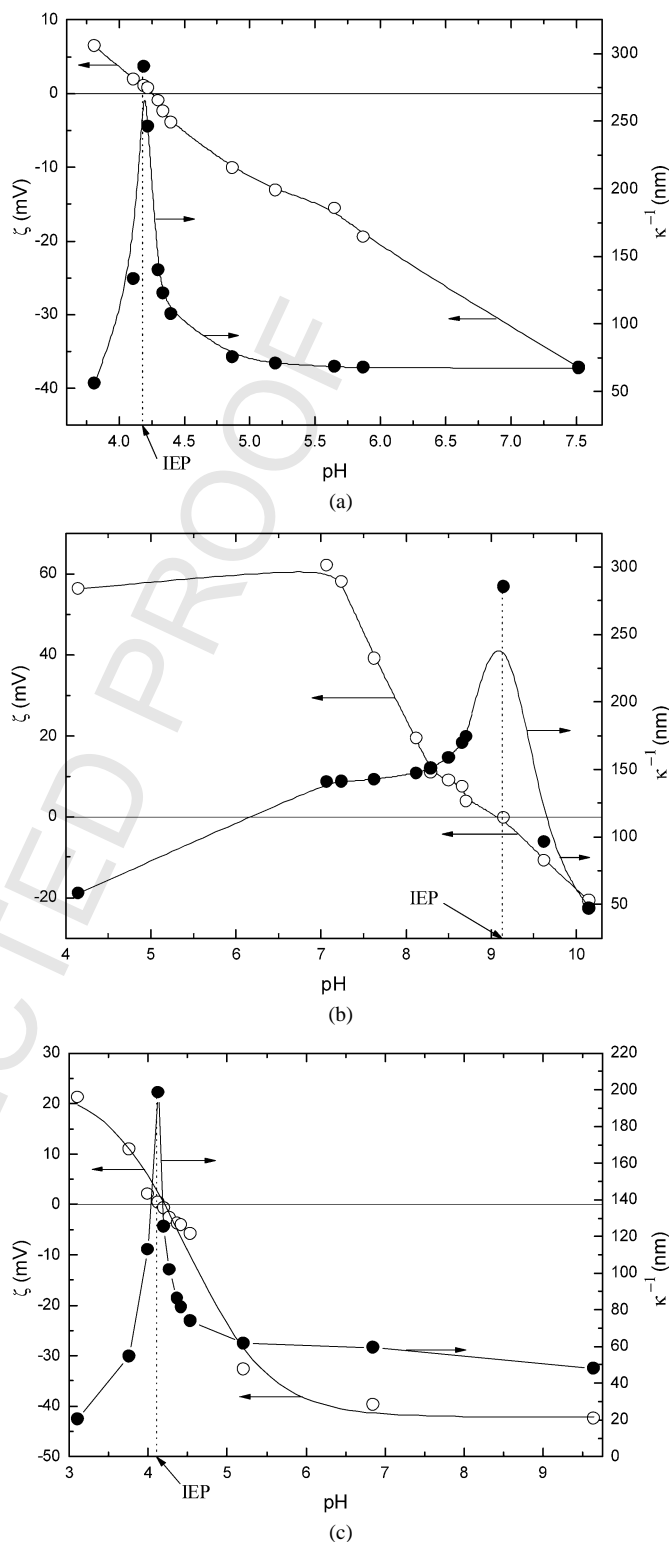


Fig. 1.  $\zeta$ -potential and  $\kappa^{-1}$  values of the suspensions of different oxides vs pH. (a) SiO<sub>2</sub>, (b) Al<sub>2</sub>O<sub>3</sub> and (c) TiO<sub>2</sub>.

mean value was taken. Although a dependence of the pH on the volume fraction exists, which results from the adsorption of potential-determining ions onto the surface of the particles, it was not appreciable at these low  $\phi$  variations, the deviation between initial and final pH values being less than 1%. As the effect of the presence of the particles on the suspension viscosity

1 is low, the uncertainties associated with the manual determina-  
2 tion of the efflux time in the viscometers may easily mask the  
3 actual viscosity variations. For this reason we have used an au-  
4 tomatic system for recording the time (AVS310, Schött-Gerate).  
5 Strong sonication was given to the samples before measuring  
6 (at least 30 min sonication was necessary for silica in order to  
7 obtain reproducible results). After each dilution the suspension  
8 was stirred with a magnetic stirring rod, before a new measure-  
9 ment of the efflux time was started. The measurements with  
10 the rheometer RS600 were performed in control stress mode.  
11 Cone-plate geometry was used. The diameter of the titanium  
12 cone and plate was 60 mm, and the angle of the cone was 1°.

13 The pH of the suspensions was measured with a pH-meter  
14 (GLP22, Crison) by using a special probe for “difficult” sam-  
15 ples (52-21, Crison).

16 To obtain the dynamic viscosity of a suspension it is neces-  
17 sary to know its density. This magnitude was obtained with a  
18 DMA-58 densimeter (Anton Paar).

19 All experiments were performed at 25 °C.

### 20 3. Results and discussion

21 The viscosity of a very dilute hard particles suspension,  $\eta$ , is  
22 greater than that of the solvent,  $\eta_0$ . This effect was theoretically  
23 predicted by Einstein [7] and it is expressed as

$$24 \eta = \eta_0(1 + [\eta]\phi). \quad (2)$$

25 In this equation  $[\eta]$  is the intrinsic viscosity, which takes the  
26 value 2.5 for spherical and uncharged particles and higher val-  
27 ues when this geometric condition is not accomplished [6].  $\phi$  is  
28 the volume fraction of solid particles in the suspension. The va-  
29 lidity of Eq. (2) is limited to an extremely diluted suspension  
30 of uncharged particles. If one of these two conditions is not ac-  
31 complished, this equation must be modified.

32 Several expressions [14–19] have been proposed to express  
33 the effect of an increase of the solid volume fraction on the vis-  
34 cosity of a hard particles suspension. However a power series  
35 in  $\phi$ , that takes into account the particle–particle interactions at  
36 several orders, was shown valid for the discussion of the exper-  
37 imental results [18],

$$38 \eta = \eta_0(1 + [\eta]\phi + K[\eta]^2\phi^2 + O(\phi^3) + \dots), \quad (3)$$

39 where  $K$  is the Huggins coefficient.

40 Von Smoluchowski [6] proposed an expression that takes  
41 into account the resistance of ionic atmosphere (the electrical  
42 double layer) that surrounds the particles against fluid distor-  
43 tion of shear. This is known as the primary electroviscous effect.  
44 Equation (1) is Smoluchowski’s result, now  $[\eta](1 + p)$  being  
45 the intrinsic viscosity of the colloidal suspension. Following  
46 Adachi et al. [20], we can distinguish between the intrinsic  
47 viscosity when the electrical effects are not manifested (hard  
48 particles), and that when the electroviscous effects are present.  
49 They are related as

$$50 [\eta]_{\text{EEV}} = [\eta](1 + p). \quad (4)$$

51 The primary electroviscous coefficient,  $p$ , was obtained by  
52 Booth [21] for arbitrary double layer thickness but limited to

53 small surface potentials,

$$54 p = q^* \left( \frac{e\zeta}{kT} \right)^2 Z(\kappa a)(1 + \kappa a)^2. \quad (5)$$

55 Here,  $e$  is the proton charge,  $\zeta$  the zeta or electrokinetic poten-  
56 tial,  $k$  the Boltzmann’s constant,  $T$  the absolute temperature,  
57 and  $Z(\kappa a)$  the relaxation function given by Booth [21]. The  
58 electrokinetic radius,  $\kappa a$ , is the ratio of the particle radius  $a$  to  
59 the screening Debye length,

$$60 \frac{1}{\kappa} = \sqrt{\frac{\epsilon kT}{\sum_{i=1}^N z_i^2 e^2 n_i}}, \quad (6)$$

61 where  $\epsilon$  is the permittivity of the liquid medium and  $n_i$  and  $z_i$   
62 are the numeric concentrations and the valences, respectively,  
63 of the  $N$  ionic species in the solution, far away from any partic-  
64 le. Finally, the term  $q^*$  is given by

$$65 q^* = \frac{6\epsilon kT \sum_{i=1}^N n_i z_i^2 / \omega_i}{e\eta_0 \sum_{i=1}^N n_i z_i^2}, \quad (7)$$

66 where  $\omega_i$  is the mobility of the  $i$ -type ion. The calculation of  
67 the sums is not evident. A controversy on the actual electrolyte  
68 concentration in a colloidal suspension has grown in colloid dis-  
69 cussions. The idea of ion condensation near the surface particle  
70 due to its surface charge has now been considered. In line with  
71 this model, a hypothesis on the electrical double layer ion con-  
72 centration was established elsewhere [22]. It is supposed that  
73 the surface charge is entirely screened or neutralised at the IEP,  
74 and there is no EDL that surrounds the particles at this pH  
75 value. The basic idea that supports this hypothesis is that at the  
76 IEP the continuum is a saturated system of ions with the same  
77 distribution at the particle surface than into the bulk. The col-  
78 loidal particles are immersed into this continuum. Therefore, at  
79 the IEP the liquid phase of the suspension will be considered  
80 as the blank reference. Consequently, when  $\text{pH} \neq \text{pH}_{\text{IEP}}$ , the  
81 differences  $\Delta\text{pH} = \text{pH} - \text{pH}_{\text{IEP}}$  and  $\Delta\text{pOH} = \text{pOH} - \text{pOH}_{\text{IEP}}$ ,  
82 together with the background electrolyte concentration, will de-  
83 termine the charge in the EDL (Fig. 2). Taking into account this  
84 hypothesis on the ion concentration in the EDL, Booth’s coeffi-  
85 cient takes the form:

$$86 p = \frac{6e\epsilon\zeta^2}{\eta_0 kT} Z(\kappa a)(1 + \kappa a)^2$$

$$87 \times \left[ \frac{\frac{|10^{-\text{pH}} - 10^{-\text{pH}_{\text{IEP}}}|}{\omega_{\text{H}}} + \frac{|10^{-\text{pOH}} - 10^{-\text{pOH}_{\text{IEP}}}|}{\omega_{\text{OH}}} + \frac{C_{\text{M}}}{\omega_{\text{M}}}}{|10^{-\text{pH}} - 10^{-\text{pH}_{\text{IEP}}}| + |10^{-\text{pOH}} - 10^{-\text{pOH}_{\text{IEP}}}| + C_{\text{M}}} \right] \quad (8)$$

88 and the screening Debye length,

$$89 \frac{1}{\kappa} = \sqrt{\frac{\epsilon kT}{e^2 N_{\text{A}} 10^3 [C_{\text{M}} + |10^{-\text{pH}} - 10^{-\text{pH}_{\text{IEP}}}| + |10^{-\text{pOH}} - 10^{-\text{pOH}_{\text{IEP}}}|]}}, \quad (9)$$

90 where  $C_{\text{M}}$  is the molar concentration of the counter-ion added  
91 to the suspension and  $N_{\text{A}}$  is the Avogadro number.

92 It is worthy to emphasise that, in these models on the viscosi-  
93 ty of suspensions, the effect of the agglomeration of particles  
94 is not taken into account. A completely dispersed suspension is

assumed in all cases. However, it is well known that clusters are formed in the particle suspensions. Depending on the particle–particle and the particle–liquid phase interactions, the shape and size of the clusters will vary. We can accept that the difference with respect to a suspension of single particles is the size and the shape of the new entities that can move through the liquid phase when a flow field is established. Really, the existence of this particle structure gives place to non-Newtonian behaviours (shear-thinning, shear-thickening, thixotropy, viscoelasticity), but only at high or moderate particle concentrations. Because we have studied very dilute suspensions, these non-Newtonian effects have not been observed.

The viscosity of  $\text{SiO}_2$ ,  $\text{Al}_2\text{O}_3$  and  $\text{TiO}_2$  suspensions, at different pH and solid volume fractions, has been measured. In Fig. 3, the inherent viscosity is plotted against the volume fraction of silica particles. As can be seen in this figure, the electroviscous effects appeared more clearly for the systems far from the isoelectric point, where the electrical double layers are thicker (Fig. 1a). That is, when the pH is more different from the IEP, the intrinsic viscosity which is the intercept of the extrapolation of the plot at  $\phi = 0$  will increase, and the slope of the curve, which reflects the presence of second order effects,

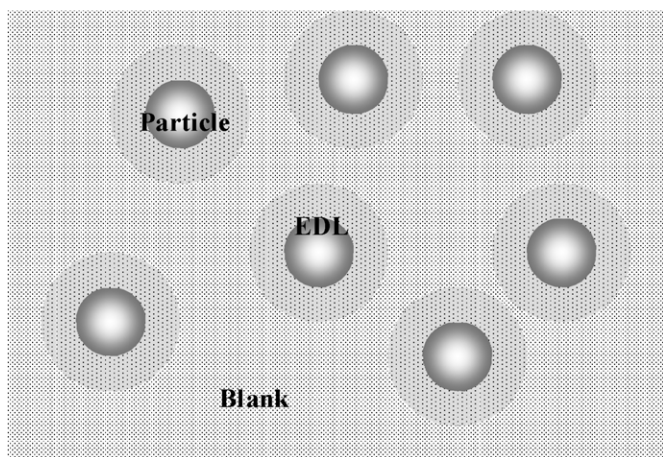


Fig. 2. The hypothesis on the electrical double layer ion concentration.

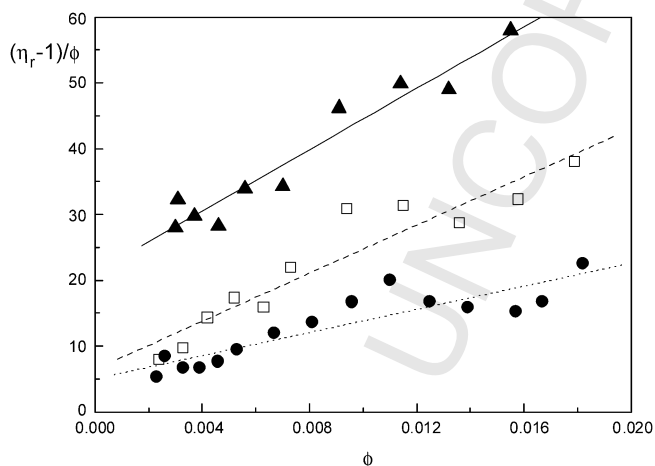


Fig. 3. Inherent viscosity of  $\text{SiO}_2$  suspensions at different pH values: ( $\blacktriangle$ ) pH 6.1, ( $\square$ ) pH 2.6, ( $\bullet$ ) pH 4.9.

also increase. In Fig. 4, the inherent viscosity of aqueous alumina suspensions is plotted against the solid volume fraction. Again, the electroviscous effects are more evident in systems far from the IEP, where  $\kappa$  decreases and  $\zeta$  increases (Fig. 1b). However, in this case, only primary electroviscous effect has been observed, as can be deduced from the zero slopes of the curves. The effect of double layer interaction is negligible in these very dilute suspensions ( $\phi \leq 0.5\%$ ). From the extrapolation of the plot at  $\phi = 0$ , the  $[\eta]_{\text{EEV}}$  values have been obtained. Finally, in Fig. 5, the specific viscosity of aqueous anatase suspensions has been plotted against the solid volume fraction, this last magnitude being less than 1%. The results suggest, like with alumina suspensions, that only primary electroviscous effect is present in these systems. Again, the electrical double layer thickness increases the higher is the difference between the pH of the suspension and the IEP (Fig. 1c). The intrinsic viscosity when the primary electroviscous effect is present is obtained from these experimental results. In all cases, a correlation between the electrical double layer thickness, the  $\zeta$ -potential values and the intrinsic viscosity of the suspensions have been obtained.

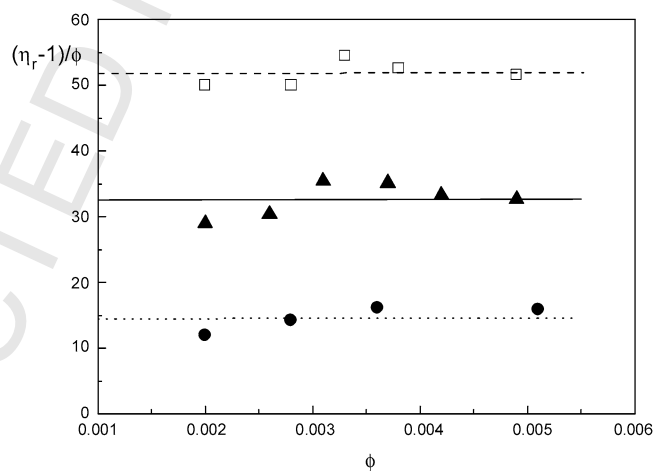


Fig. 4. Inherent viscosity of  $\text{Al}_2\text{O}_3$  suspensions at different pH values: ( $\square$ ) pH 11.4, ( $\blacktriangle$ ) pH 6.3, ( $\bullet$ ) pH 7.9.

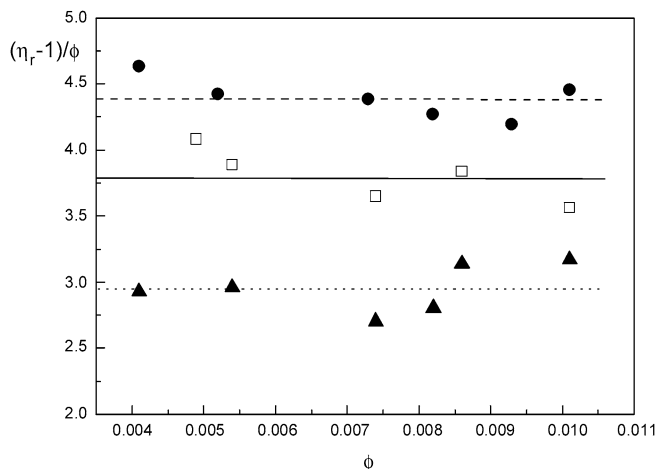


Fig. 5. Inherent viscosity of  $\text{TiO}_2$  suspensions at different pH values: ( $\bullet$ ) pH 5.9, ( $\bullet$ ) pH 4.7, ( $\blacktriangle$ ) pH 4.2.

Table 2

Booth's primary electroviscous coefficient, the intrinsic viscosity, the axial ratio of the equivalent ellipsoid of revolution, and the particle volume fraction in a cluster

Material	$\Delta\text{pH}$	$p_{\text{Booth}}$	$[\eta]$	$a/b$	$\phi_{\text{pc}}$
SiO <sub>2</sub>	1.8	0.0065	20.9	13.5	0.120
	1.7	0.0022	6.3	5.5	0.397
	0.6	0.0018	5.7	5.0	0.439
Al <sub>2</sub> O <sub>3</sub>	2.8	0.029	32.1	15.9	0.078
	2.3	0.245	41.8	20.0	0.060
	1.2	0.007	14.9	10.5	0.168
TiO <sub>2</sub>	2.4	0.135	3.8	3.2	0.658
	1.2	0.082	3.5	3.0	0.714
	0.7	0.047	2.8	1.2	0.893

The primary electroviscous coefficient has been calculated by using Booth's equation [21]. The validity of Booth's model has been tested [3,22] and it has been assumed in this work. In Table 2 Booth's primary electroviscous coefficient and the intrinsic viscosity, obtained by using Eq. (4) and the experimental  $[\eta]_{\text{IEV}}$  values, are shown.

As can be seen, except in one case, the intrinsic viscosity increases when  $\Delta\text{pH} = |\text{pH} - \text{pH}_{\text{IEP}}|$  increases. On the other hand, a correlation has been found between the  $p$ -value and the intrinsic viscosity. The higher the  $p$ -value, the higher the intrinsic viscosity.

The fact that, in absence of electroviscous effects, the intrinsic viscosity was pH-dependent can be explained as follows. The shape of the clusters that may be formed in these suspensions, moving in the flow field, determines the value of the intrinsic viscosity. This magnitude is dependent on the shape of the kinetic unity [23]. Smith and Bruce [10] established a correlation between the intrinsic viscosity and the shear rate applied to suspensions of  $\alpha\text{-Fe}_2\text{O}_3$  and  $\gamma\text{-Fe}_2\text{O}_3$ . These authors obtained that the intrinsic viscosity of the suspension decreases with the shear rate. At low shear rates the suspension is more structured forming a network. At high shear rates the shape of the clusters that are formed from the rupture of the network become more and more spherical when the shear rate increases [24]. Therefore the intrinsic viscosity tends to the minimum value when the shear rate increases. In our case, the shape of the clusters is pH-dependent, because the repulsive electrical energy between particles is related to the variation of this parameter. Near the IEP the repulsive force between particles reduces [25], as can be deduced from the  $\zeta$ -potential and  $\kappa$  values that are shown in Figs. 1a–1c, allowing particles to group in aggregates easily.

Silica particles are spherical, but it is well known that they form aggregates by hydrogen bridges due to the interaction of the silanol groups that form onto its surface. When the electrical repulsive energy is high, far from the IEP, the form of the cluster tends to be a chain. When the electrical repulsive energy is low, near the IEP, the form of the cluster tends to be a sphere. These two last claims are supported by the calculations which were made following Biddle et al. [26]. In this reference a method is proposed to obtain an estimation of the shape and size of particle aggregates. To apply their method it is necessary to combine

viscosity and dynamic scattering light measurements (or other similar methods to measure hydrodynamics characteristics of the system) [27, pp. 327, 335]. Then, the axial ratio of an ellipsoid of revolution which is equivalent to the particle aggregate and the values of its axis are obtained. Although we have not in our laboratory a device which can allow us to make dynamic scattering light measurements, only with the intrinsic viscosity data and Simha's plots [27, pp. 335–336], we can determine the axial ratio of the equivalent ellipsoid. The results are shown in Table 2. As can be seen, this magnitude decreases near the IEP, suggesting a less "prolate" ellipsoid.

Alumina particles have a very irregular shape. Near the IEP, the particles form aggregates with a more spherical shape than an isolated particle, but far of this point they tend to form more elongated clusters, as can be deduced from the axial ratio which was calculated following the method by Biddle et al. [26]. The results are shown in Table 2.

Finally, isolated anatase particles are almost spherical. In this case, a very large variation in the intrinsic viscosity due to the formation of clusters is not expected. This is due to that the clusters will tend to be more and more spherical near the IEP, like the isolated particles. The clusters with a very spherical form do not modify the intrinsic viscosity value, because, as was pointed out by Einstein,  $[\eta] = 2.5$  independent of the size of the spherical particle. So both near and far from the IEP the intrinsic viscosity should tend to be 2.5 for the anatase suspensions. The results in the Table 2 show that the deviation from this value is small enough to accept the validity of this argument. Moreover, the axial ratio of the equivalent ellipsoid [26] tends to 1 at the IEP, which confirms this description. It is clear that the clusters have a light elongated form far from the IEP.

It is also interesting to determine the compaction of a cluster. In studies on the structure dependence of rheological behaviours (shear-thinning, shear-thickening, thixotropy, etc.) a determining parameter was shown [24,28–30]. From the intrinsic viscosity values, the volume fraction of particles in a cluster can be obtained using the relation derived by Smith and Bruce [10],

$$[\eta] = \frac{2.5}{\phi_{\text{pc}}} \quad (10)$$

The particle volume fraction in a cluster,  $\phi_{\text{pc}}$ , is the quotient between the volume fraction of particles in the suspension,  $\phi$ , and the volume fraction of clusters  $\phi_{\text{c}}$ . It is clear that the higher the intrinsic viscosity of the suspension, the lower the particle volume fraction in a cluster. This is a consistent result with the formation of chains of particles far from the IEP: obviously, in these clusters,  $\phi_{\text{pc}}$  should be lower than for the more spherical clusters that form near the IEP.

## Acknowledgments

Financial support by CICYT (Spain), project no. MAT2003-04688 is gratefully acknowledged. We thank Vicerrectorado de Investigación (University of Málaga, Spain) for support during this research.

## References

- [1] J. Stone-Masui, A. Watillon, *J. Colloid Interface Sci.* 28 (1968) 187.
- [2] E.P. Honig, W.F.J. Pünt, P.H.G. Offermans, *J. Colloid Interface Sci.* 134 (1990) 169.
- [3] J. Yamanaka, N. Ise, H. Miyoshi, T. Yamaguchi, *Phys. Rev. E* 51 (1995) 1276.
- [4] F.J. Rubio-Hernández, A.I. Gómez-Merino, E. Ruiz-Reina, C. Carnero-Ruiz, *Colloids Surf. A* 140 (1998) 295.
- [5] I.G. Watterson, L.R. White, *J. Chem. Soc. Faraday Trans.* 77 (1981) 1115.
- [6] M. Von Smoluchowski, *Kolloid Z.* 18 (1916) 190.
- [7] A. Einstein, *Ann. Phys.* 34 (1911) 591.
- [8] E.J.W. Verwey, J.Th.G. Overbeek, *Theory of the Stability of Lyophobic Colloids*, Elsevier, Amsterdam, 1948.
- [9] B.V. Derjaguin, L.D. Landau, *Acta Physicochim. USSR* 14 (1941) 633.
- [10] T.L. Smith, C.A. Bruce, *J. Colloid Interface Sci.* 72 (1979) 13.
- [11] J. Gustafsson, P. Mikkola, M. Jokinen, J.B. Rosenholm, *Colloids Surf. A* 175 (2000) 349.
- [12] Z.Z. Zhang, D.L. Sparks, N.C. Scrivner, *J. Colloid Interface Sci.* 162 (1994) 244.
- [13] H. Ohshima, in: H. Ohshima, K. Furusawa (Eds.), *Electrical Phenomena at Interfaces. Measurements and Applications*, Dekker, New York, 1998.
- [14] R. Simha, *J. Appl. Phys.* 23 (1952) 1020.
- [15] M. Mooney, *J. Colloid Sci.* 6 (1957) 162.
- [16] I.M. Krieger, T.J. Dugherty, *Trans. Soc. Rheol.* 3 (1959) 137.
- [17] J.S. Chong, E.B. Christiansen, A.D. Baer, *J. Appl. Polym. Sci.* 15 (1971) 2007.
- [18] G.K. Batchelor, *J. Fluid Mech.* 83 (1977) 97.
- [19] W.B. Russel, *J. Fluid Mech.* 85 (1978) 209.
- [20] Y. Adachi, K. Nakaishi, M. Tamaki, *J. Colloid Interface Sci.* 198 (1998) 100.
- [21] F. Booth, *Proc. R. Soc. London Ser. A* 203 (1950) 533.
- [22] F.J. Rubio-Hernández, A.I. Gómez-Merino, E. Ruiz-Reina, P. García-Sánchez, *J. Colloid Interface Sci.* 255 (2002) 208.
- [23] H. Brenner, *Int. J. Multiphase Flow* 1 (1974) 195.
- [24] D. Quemada, *Eur. Phys. J. Appl. Phys.* 1 (1998) 119.
- [25] F.J. Rubio-Hernández, P. Fortes-Quesada, in press.
- [26] D. Biddle, C. Walldal, S. Wall, *Colloids Surf. A* 118 (1996) 89.
- [27] C. Tanford, *Physical Chemistry of Macromolecules*, Wiley & Sons, New York, 1961.
- [28] D. Quemada, *Eur. Phys. J. Appl. Phys.* 2 (1998) 175.
- [29] D. Quemada, *Eur. Phys. J. Appl. Phys.* 3 (1998) 309.
- [30] D. Quemada, *Eur. Phys. J. Appl. Phys.* 5 (1999) 191.